

## ARTICLE OPEN



# Fully paper-integrated hydrophobic and air permeable piezoresistive sensors for high-humidity and underwater wearable motion monitoring

Yuewen Wei<sup>1</sup>, Xuewen Shi<sup>1</sup>, Zhuoqi Yao<sup>1</sup>, Jiakai Zhi<sup>1</sup>, Lixuan Hu<sup>1</sup>, Ren Yan<sup>1</sup>, Chuanqian Shi<sup>2</sup>✉, Hai-Dong Yu<sup>1</sup>✉ and Wei Huang<sup>1</sup>✉

Paper-based electronics have attracted much attention due to their softness, degradability, and low cost. However, paper-based sensors are difficult to apply to high-humidity environments or even underwater. Here, we report a fully paper-integrated piezoresistive sensing system that exhibits flexibility, waterproofing, air permeability, and biocompatibility. This system consists of hydrophobic paper as the substrate and encapsulation layer, conductive paper with a double 'zig-zag' and dotted surface structure as the sensing layer, and silver paste films as the interconnects. The structural design of the sensing layer helps to increase the contact area in adjacent layers under pressure and further improves the pressure sensitivity. The piezoresistive system can be worn on human skin in the ambient environment, wet environment, and water for real-time monitoring of physiological signals with air permeability and waterproofing due to its hydrophobic fiber structure. Such a device provides a reliable, economical, and eco-friendly solution to wearable technologies.

*npj Flexible Electronics* (2023)7:13 | <https://doi.org/10.1038/s41528-023-00244-5>

## INTRODUCTION

The emergence of wearable electronics has promoted the development of flexible electronic devices that can be integrated into the human body for health monitoring<sup>1–5</sup>, physical tracking<sup>6–8</sup>, and human-computer interacting<sup>6,7,9</sup>. At the same time, wearable electronics will not limit the activities of human beings or machines due to their flexibility and lightness<sup>10,11</sup>. Among all the exciting applications, pressure sensors play an important role<sup>12,13</sup> as they can be widely used in many aspects, including respiratory monitoring<sup>14,15</sup>, pulse detection<sup>16,17</sup>, and other physiological signal acquisition<sup>18,19</sup>. Pressure sensors can be classified into capacitive<sup>20,21</sup>, piezoresistive<sup>22–24</sup>, piezoelectric<sup>17,25</sup>, and triboelectric<sup>26,27</sup> sensors according to different working principles. Piezoresistive sensors, in particular, have the advantages of simple operation, low energy consumption, high sensitivity in low-pressure range, and simple signal acquisition<sup>7,28</sup>.

The development of flexible electronics is related to advances in materials and mechanical designs. However, with the increasing demand for electronic products, a large number of electronic wastes and their discarded toxic substances cause serious environmental pollution<sup>29,30</sup>. The commonly used polymers are often complicated, costly, and difficult to degrade, and may cause a burden on the environment<sup>31</sup>. Some fabric-based sensors offer greater flexibility and comfort, but fabrics, which are usually made from a mixture of natural plant fibers and chemical synthetic fibers, have similar problems with natural degradation as polymers<sup>32,33</sup>. Therefore, one direction of particular interest is to integrate environmentally friendly properties in wearable electronics by exploring green materials, most of which are based on fibroin<sup>34,35</sup>, gelatin<sup>7,36</sup>, and paper<sup>37–41</sup>.

Paper-based flexible sensors have attracted a surge of interest because of their characteristics including flexibility, low cost, abundant resource, biocompatibility, and environmental

protection<sup>41–46</sup>. However, the perspiration of human skin can affect the sensing performance of the device. In some special wet environment, such as bathing and swimming conditions, waterproof performance is necessary. Therefore, most paper-based sensors tend to use non-paper packaging to protect, such as PDMS<sup>43,47,48</sup>, PI<sup>49</sup>, PTFE<sup>50</sup>, and other polymers<sup>31</sup>. However, these polymers are difficult to degrade in nature<sup>50</sup>. In addition, good breathability is also extremely important for comfortable, non-inflammatory wearable electronics<sup>51,52</sup>. Compared to other encapsulation materials, cellulose paper is a good breathable material due to its porous structure, and it will not cause discomfort even if worn on the skin for a long time<sup>53</sup>. Furthermore, the studies have confirmed that cellulose paper has good degradability and have reported the sensors based on cellulose paper with good degradability by biology and combustion<sup>41,54–56</sup>. Recently, some fully paper-based flexible sensors have been successfully constructed for the detection of human activities<sup>42,57,58</sup>, and paper with the porous microstructure had a good air permeability, but it also leads to poor water resistance of the sensor and loss of function when working in water or high humidity environments. Therefore, developing a fully paper-based sensor with waterproofing and air permeability is a challenge in terms of device performance and environmental care.

For flexible wearable paper-based sensors, we previously reported an all-paper-based pressure sensor that uses paper coated with silver nanowires as the sensing layer and transparent paper as the packaging layer<sup>42</sup>. However, the packaging paper used in this report is not waterproof, limiting its use in wet or underwater environments. Therefore, the previously reported application of all paper-based pressure sensors in some special environments remains to be solved.

In this work, we have developed an all paper-integrated flexible sensing system that is compatible with waterproofing, air

<sup>1</sup>Frontiers Science Center for Flexible Electronics, Xi'an Institute of Flexible Electronics (IFE) and Xi'an Institute of Biomedical Materials & Engineering, Northwestern Polytechnical University, 127 West Youyi Road, Xi'an 710072, China. <sup>2</sup>Key Laboratory of Impact and Safety Engineering, Ministry of Education, Ningbo University, Ningbo 315201, China.

✉email: shichuanqian@nbu.edu.cn; iamhdyyu@nwpu.edu.cn; iamwhuang@nwpu.edu.cn

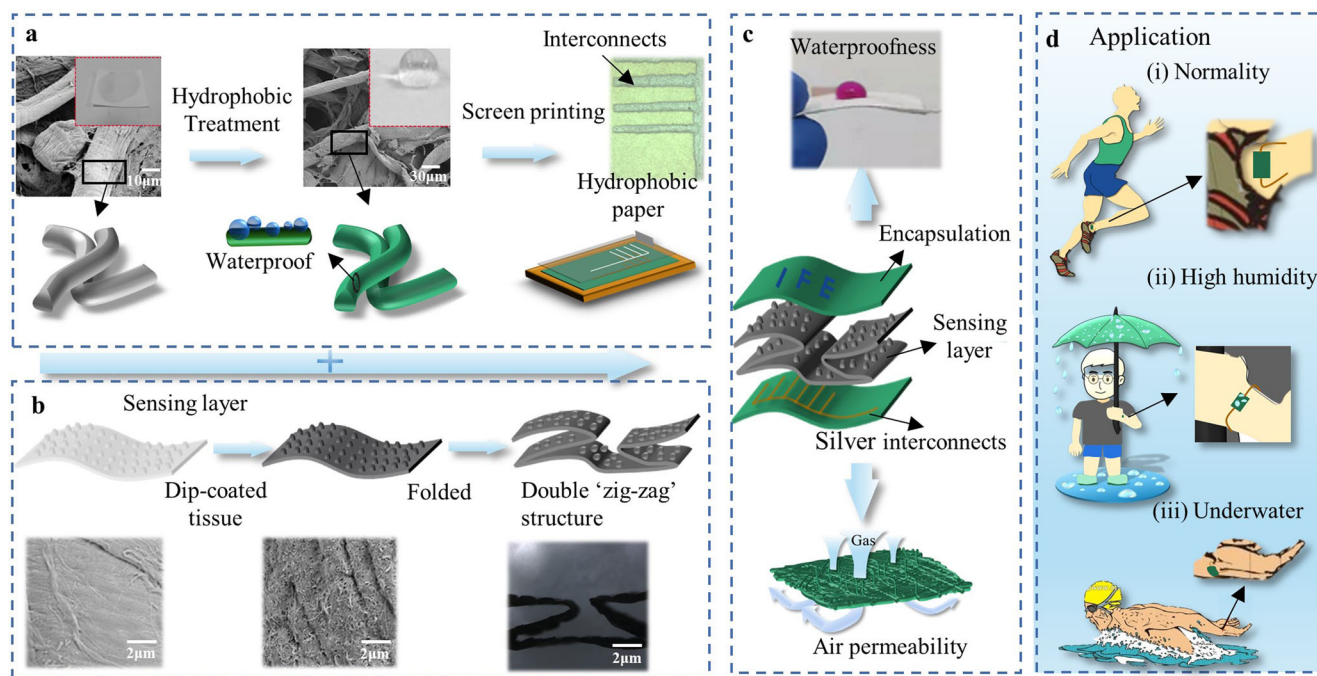


**Fig. 1** Illustration for the fabrication and applications of a fully paper-based flexible piezoresistive sensing system. **a** Preparation of hydrophobic paper and screen printing of the interconnects. **b** Preparation of the sensing layer with dotted surface and double 'zig-zag' structure. **c** Schematic diagram of the integrated flexible piezoresistive sensor and its hydrophobicity and air permeability. **d** Different application scenarios of the flexible piezoresistive sensing system, including Normal (i), high-Humidity (ii), and Underwater (iii) conditions. (This image does not contain any third party material).

permeability, and eco-friendly. The piezoresistive sensing system consists of three components: hydrophobic and air permeability paper as flexible encapsulations, a conductive paper with a double 'zig-zag' structure and a dotted roughed surface as a sensing layer, and the silver paste films as the interconnects between the encapsulation and sensing layer. Due to the structural design of the sensing layer, the obtained pressure sensor exhibits sensitivity of  $12.6 \text{ kPa}^{-1}$  and  $4.3 \text{ kPa}^{-1}$  under the pressure between high detection range of 0 to 0.6 kPa and 0.6–60.4 kPa, respectively, and the fully paper-based sensor has low working voltage and fast response time. Such pressure systems can also be easily disposed of by incineration. The flexible piezoresistive sensing system has been successfully applied to monitor human physiological signals, including finger touch and bending, sitting posture, arterial pulse, acoustic sounds, and walking signals. Besides the detections under ambient conditions, the successful underwater applications demonstrate the water-proofing ability of the piezoresistive system. We believe that the proposed flexible piezoresistive sensing system will be applied in many complex scenarios such as medical treatment, daily life, shallow water environment, and rainy days. This work will pave the way for manufacturing low-cost and easy-to-use paper-based hydrophobic sensors and broaden their application scope, and will promote the development of green flexible electronics.

## RESULTS AND DISCUSSION

### Design and fabrication of fully paper-based flexible piezoresistive sensor

The sandwich structure piezoresistive sensor consists of conductive paper as the sensing layer and hydrophobic paper with silver interconnects as the packaging layer. Figure 1a and Supplementary Fig. 4a demonstrate the hydrophobic treatment process by evaporating the methyl trichlorosilane gas into the filter paper in a vacuum oven at  $45^\circ\text{C}$ . An original filter paper (Fig. 1a, left inset)

made up of non-waterproof fibers (Fig. 1a, left) is treated with methyl trichlorosilane vapor, and methyl trichlorosilane reacts with the hydroxyl groups on the fiber and replaces hydrophilic groups on the fibers' surface (Fig. 1a, middle, Supplementary Fig. 4c, d), which makes the paper hydrophobic (Fig. 1a, middle inset). Scanning electron microscope (SEM) images show that the fibers changes from the original smooth surface (Supplementary Fig. 5a) to rough surface (Supplementary Fig. 5b) when treated with methyl trichlorosilane, which proves that methyl trichlorosilane is uniformly bonded to the fibers, changing the hydrophilicity of the fibers. At the same time, the static contact angle and rolling contact angle of the hydrophobic paper were characterized. On the original paper, dripping water droplets would be rapidly absorbed, while on the surface of the hydrophobic paper, the contact angle was about  $143^\circ$  (Supplementary Fig. 5c). As shown in Supplementary Fig. 6, the hydrophobic paper with a drop of water on the surface proves that the paper remains hydrophobic when subjected to different bending conditions. When  $10 \mu\text{L}$  of water drops from a height of 4 cm, the surface of the hydrophobic paper tilts at least  $38^\circ$ , which indicates that the rolling contact angle of the hydrophobic paper is  $38^\circ$  (Supplementary Fig. 5d). Simultaneously, the waterproof filter paper obtains good air permeability due to the porous nature between the fibers (Supplementary Fig. 4b). Silver paste interconnects were screen-printed on the prepared hydrophobic paper and used as electrodes attached to conductive paper to signal from the sensing layer to external devices (Fig. 1a, right). To illustrate the electric robustness of the printing wires, we connected the hydrophobic paper with interconnects into the circuit, and the brightness of the LED was unchanged under non-bending, concave bending and convex bending (Supplementary Fig. 7a–c). And when the bending angle of the hydrophobic paper was increased from 0 to 120 degrees, the resistance of the interconnects is  $\sim 0.5 \Omega$  (Supplementary Fig. 7d, e).

The sensing layer is prepared by dip coating tissue paper in the aqueous composite solutions of single-walled carbon nanotubes

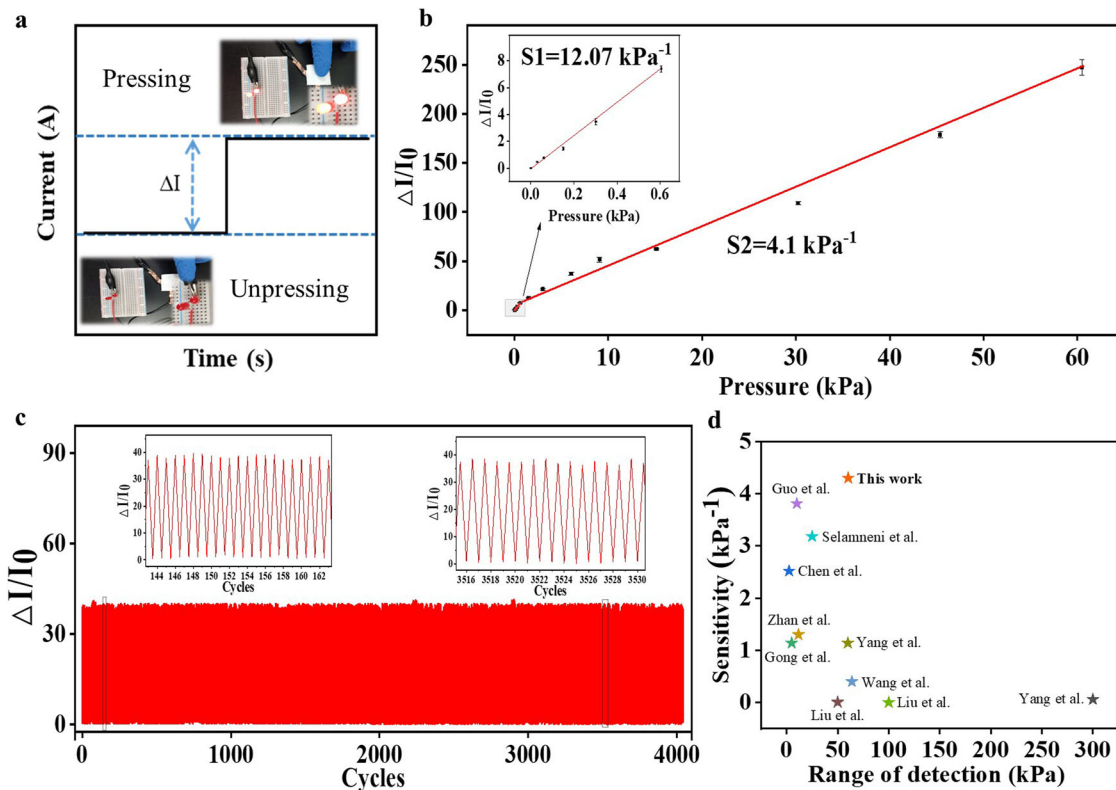


**Fig. 2** Electrical performance of the fully paper-based flexible piezoresistive sensor. **a** The currents generated when pressure loaded on the sensor, disappeared when unloaded. **b** The fractional change of current from a fully paper-based flexible piezoresistive sensor under pressing, the enlarged view in a small pressure range of 0–0.6 kPa. **c** The fractional change of current in the 4000 cycles, the enlarged diagrams for 144–162 cycles and 3517–3530 cycles. **d** Comparison of this work with currently reported paper-based pressure sensors in terms of sensitivity and range of detection.

(SWNTs) and graphene (Fig. 1b). The paper will change color from off-white to black after drying (the detailed preparation process is shown in methods and Supplementary Fig. 2b). Compared with the original fibers of tissue paper (Fig. 1b, bottom left and Supplementary Fig. 8a, b), the modified fibers are attached by graphene/SWNTs composites uniformly (Fig. 1b, bottom middle, Supplementary Fig. 8c–i). The modified conductive paper with a porous structure would respond to the applied pressure under a fixed voltage and cause regular changes in current. The folded conductive paper can lift a 200 g weight, which proves its good mechanical strength and good flexibility (Supplementary Fig. 9a). Therefore, a double ‘zig-zag’ shaped structure was folded as the final sensing layer. Besides the porous structure, the dotted surface of the tissue (Supplementary Fig. 9b, c) and double ‘zig-zag’ stack layers (Fig. 1b, right and Supplementary Fig. 10) improve the mechanotransduction sensitivity of the sensing layer due to the increasing electrical contacts between fibers in adjacent paper layers as pressing (Supplementary Fig. 9b, c)<sup>59,60</sup>. We also test the contact angle of a drop of water on the original and conductive tissue to compare their hydrophobic properties. At the very beginning, the contact angle of a droplet on the conductive tissue is larger than that of the original tissue (Supplementary Fig. 11a, d). The droplet on the original paper is absorbed gradually after 3 seconds (Supplementary Fig. 11b, c), but that on the conductive paper is still intact in 5 s, which proves the sensing layer has certain hydrophobicity (Supplementary Fig. 11e, f).

The hydrophobic paper with interconnects is used to package the sensing layer and integrated in the sandwich piezoresistive system (Fig. 1c). In addition, the hydrophobicity of the encapsulation and sensing layer ensures the potential of underwater application of the piezoresistive system (Fig. 1c, up), and the porous network structure of the conductive and hydrophobic

paper also makes the sensor have an air permeability, which indicates a potential biocompatibility (Fig. 1c, bottom). Benefiting from the hydrophobicity, air permeability, and higher mechanotransduction sensitivity, the fully paper-based piezoresistive sensing system has the capability of being applied under ambient condition, high-humidity environment, and underwater (Fig. 1d).

#### Electrical properties of the fully paper-based flexible piezoresistive sensor

We demonstrate the current generation and disappearance with and without finger pressing, respectively, due to the structural deformation of the sensing layer, in which the brightness and darkness of the LED in the insets also illustrate such phenomenon (Fig. 2a). As the increase of pressure in a wide pressure range of 0.03–60.4 kPa, the fractional change of current ( $\Delta I/I_0$ ) has increased accordingly (Supplementary Fig. 12a). As shown in Fig. 2b and its inset, the fully paper-based piezoresistive sensor has a high sensitivity of 12.6  $\text{kPa}^{-1}$  and 4.3  $\text{kPa}^{-1}$  in a range of 0.03–0.6 and 0.6–60.4, respectively. Specifically, the pressure sensitivity can be defined as the formula  $S = \delta(\Delta I/I_0)/\delta P$ , where  $P$  is the applied pressure<sup>42,61,62</sup>. The high sensitivity of the sensing layer is attributed to the double ‘zig-zag’ folded stacks, a certain number of rough dotted on the surface, and the porous nature of paper fibers. When subjected to the external pressure, both the decrease of the angle on ‘zig-zag’ folded structures and the mutual squeeze between the dots on the surface can lead to the increase of the contact area in the adjacent layers, while the reduction of the fibers gap also increases the contact area inside the sensing layer. The growth of the contact area will result in a significant decrease in the resistance, that is, a noticeable increase in current variation  $\Delta I$ , thus rising the sensitivity  $S$ .

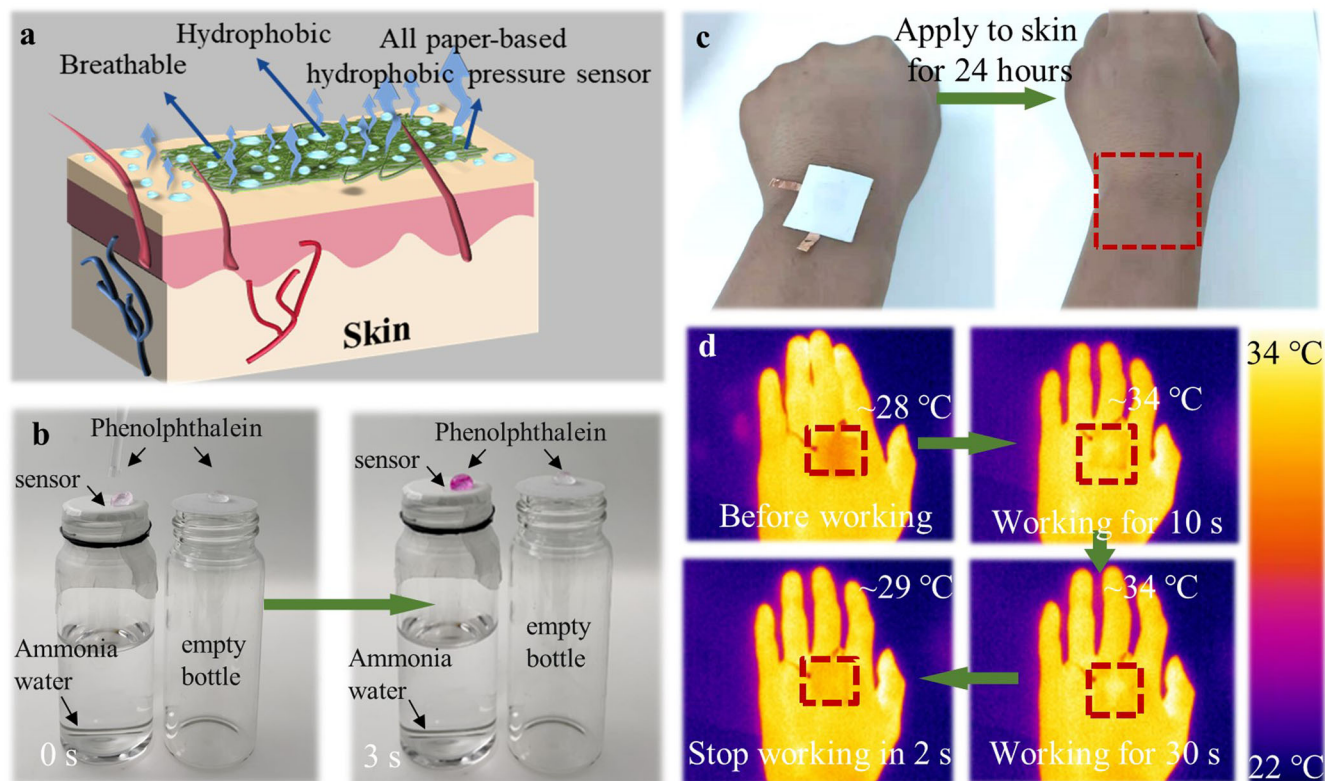


**Fig. 3** Hydrophobic and air permeable properties of the fully paper-based flexible piezoresistive sensor. **a** Schematic diagram of a sensor attached to human skin with air permeable and hydrophobic effects. **b** Air permeability test of the flexible piezoresistive sensor. **c** A photograph of the piezoresistive sensor worn on the skin (left) and a photograph of the skin after wearing it for 24 hours (right). **d** Infrared images of the sensor before working (top left), working for 10 seconds (top right), working for 30 seconds (bottom right), and stopping working in 2 seconds (bottom left).

Supplementary Fig. 12b proves that the sensitivity of our sensing layer is much higher than that of a non-stacked sensing layer (P1) and a smooth surface sensing layer (P2), in which the materials and manufacturing processes of the three sensors are the same.

It is worth mentioning that such pressure sensor modified by graphene/SWNTs also has good resilience when unloaded because the folded paper with the angles is more likely to spring back, and the surface dots treated with conductive materials are more elastic. As proved by the cyclic test in Fig. 2c, the response of the piezoresistive sensor in 4000 cycles loading/unloading under constant pressure and frequency represents outstanding repeatability and stability, and the enlarged diagrams of 144–162 cycles in the earlier period and 3517–3530 cycles in the later period illustrate no significant difference as shown in the insets in Fig. 2c. As investigated in Supplementary Fig. 13a, the response and recovery time grow with the increase of the loading force, but the response and recovery time are still less than 330 ms and 380 ms, respectively when the pressure is as high as 60 kPa. Compared with the previously reported paper-based piezoresistive sensing studies, this work has achieved relatively high sensitivity, large detection range and low working voltage (0.1 V) (Fig. 2d). Furthermore, unlike other encapsulations containing commercial non-degradable materials, this fully paper-based sensor is more environmentally friendly and less costly, because it takes only \$0.2 to fabricate one piezoresistive sensor.

#### Hydrophobic, air permeable, and eco-friendly properties of the fully paper-based flexible piezoresistive sensor

Besides the electrical properties, the fully paper-based sensor needs to mimic a person's skin with good flexible, waterproof, and air permeable properties, and can be easily worn on the skin

without affecting the skin's health/comfort (Fig. 3a). Therefore, the air permeability and waterproofness of the integrated sensor needs to be explored. As demonstrated in Fig. 3b, the paper-based piezoresistive sensor was put on the top of the glass bottle and the gap of the bottle and piezoresistive sensor was sealed by parafilm (PM996, PARAFILM) and rubber band. We also prepared an empty bottle as a control group. Phenolphthalein solution was added to the exposed paper-based piezoresistive sensor. The evaporation of the ammonia solution changed the color of the phenolphthalein droplets at the mouth of the bottle from transparent to dark red, while the phenolphthalein droplet of control group did not change color, which indicated that the sensor had good air permeability. At the same time, the trichloromethane treated paper has good hydrophobicity and does not cause biological hazards<sup>63</sup>. In order to verify the water resistance, we placed the hydrophobic paper of the sensor with a drop of water on the top of pH test paper for 12 hours, and the pH test paper did not change color because of no water penetration (Supplementary Fig. 13b). The good waterproof and air permeable properties are attributed to the modified hydrophobic fibers and the porous nature of this fully paper-based sensor. In Fig. 3c, the skin of a volunteer was compared before and after wearing the waterproof, breathable paper-based sensor for 24 hours, and no significant changes to the skin were observed, proving that the paper-based sensor had no effect on the skin. As photographed by infrared radiation (IR) camera in Fig. 3d, the temperatures of the sensor worn on the skin were ~28 °C, 34 °C, 34 °C, and 29 °C before working, working for 10 seconds and 30 seconds, and stop working for 2 seconds, respectively. The results showed that the sensor has fast heat dissipation and good heat diffusion performance because the thin thickness and

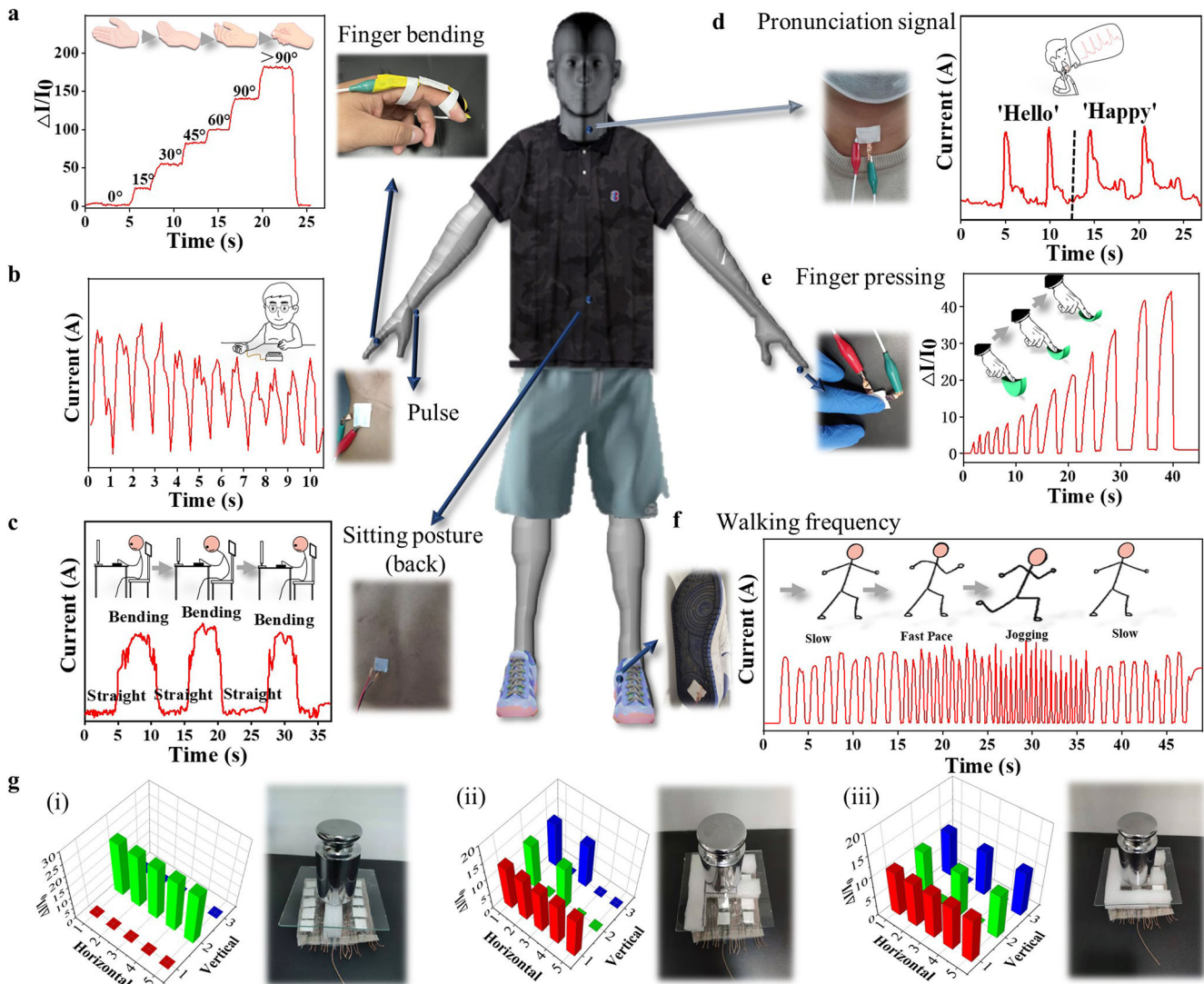


**Fig. 4 Application in real-time monitoring of human physiological signals.** **a** The real-time response of the sensor fixed on the index finger at different bending angles. The photo is an optical image of the sensor worn on a finger. **b** The pulse on the wrist measured by the sensor at a rate of 72 beats per minute. The photo is an optical image of the sensor worn on the wrist. **c** The real-time response of the sensor fixed on the back of the human body in different sitting positions. The photo is an optical image of the sensor attached to the back. **d** Response curves of the sensor mounted on the throat to monitor voice pronunciation. The photo is an optical image of the sensor worn on the throat. **e** The real-time response of the sensor during finger pressing. The photo is an optical image of the sensor under finger pressing. **f** Real-time response of the sensor mounted on a foot at different walking frequencies. The photo is an optical image of the sensor attached to a shoe. **g** The sensing array response mapping of the pressure distributions corresponding to different shapes of 'l' (i), 'F' (ii), and 'E' (iii) and their optical images.

porous structure of paper help the sensor dissipate heat when attached to human skin. As shown in Supplementary Fig. 14, the sensor is easily ignited and can quickly be carbonized in the air and then reduced to ash by slight crushing. Unlike sensors made from metal and polymer materials such as copper<sup>64,65</sup>, PET<sup>66,67</sup>, and PDMS<sup>43,47</sup>, this fully paper-based sensor can be easily treated by microbial degradation or incineration<sup>42</sup> when damaged or no longer needed.

#### Detection of physical signals with the fully paper-based flexible piezoresistive sensor under ambient conditions

Due to the sensitivity and stability of the piezoresistive sensor, we have explored applications of the sensor and demonstrated its potential as a wearable device for testing physiological signals and detecting human activities. The compliant paper-based sensor reported here can capture a wide range of pressure on

human skin and thus can be attached to different parts of the human body for different purposes. Figure 4a demonstrates a piezoresistive sensor attached to an index finger for monitoring its degree of flexion. Six different bending states of finger flexion can be accurately captured by the piezoresistive sensor from an angle of 0° to >90°. Figure 4b presents pulse monitoring data from the piezoresistive sensor attached to the wrist of a male adult (75 kg, 24 years old), with a frequency of 72/min. Such information can be used to detect abnormalities in the rate of pulse, which are a strong indicator of acute events, such as arteriosclerosis<sup>68,69</sup>, myocardial infarction<sup>70</sup>, coronary heart disease<sup>71,72</sup>, ischemic heart disease, and stroke<sup>73</sup>. The piezoresistive sensor can also be attached to the back to detect the sitting postures to help remind users sedentary position and to change it in time (Fig. 4c). As shown in Fig. 4d, the pronunciation signal can be monitored by a piezoresistive sensor worn on the throat, because the muscle movements from throat will produce

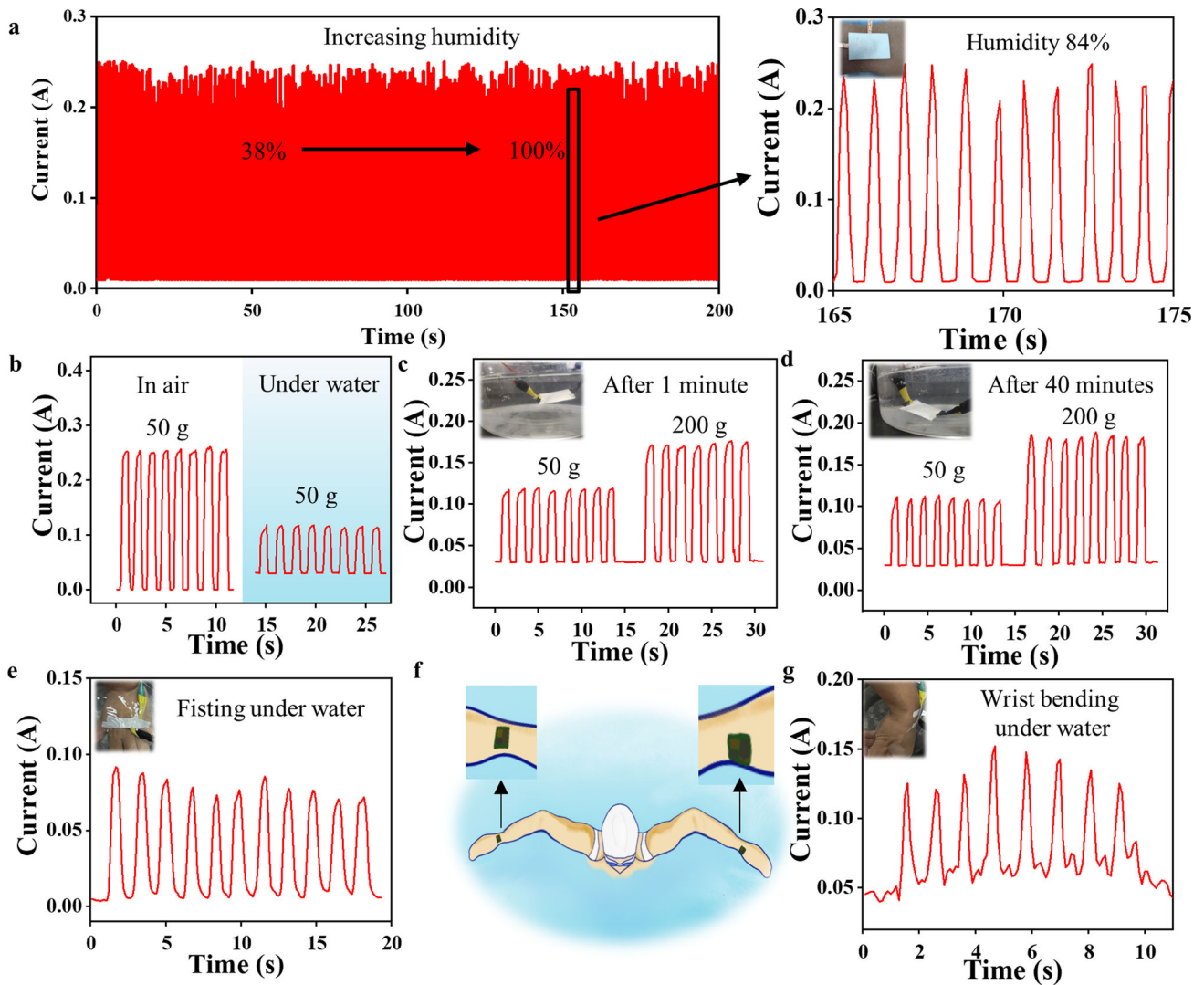


**Fig. 5 Application of fully paper-based flexible piezoresistive sensor in high humidity and water environment.** **a** Cyclic tests of the sensor under continuously changing environmental conditions of humidity (room humidity: 38–100%), the enlarged data of a piezoresistive sensor in 84% humidity environment, the inset is an optical image demonstrates the sensor attached on the wrist in this test. **b** Cyclic tests of the sensor at 50 g weight in air and underwater environments. **c** Pressure response of the sensor after 1 minute in water (left: 50 g; right: 200 g). **d** Pressure response of the sensor after 40 minutes in water (left: 50 g; right: 200 g). **e** The fisting response of the wrist under water taken by piezoresistive sensor. **f** Schematic diagram of sensors for monitoring human motions during swimming. **g** The bending response of the wrist under water taken by a flexible piezoresistive sensor.

pressure on the sensor. The data captured show distinct signatures of different verbal commands as the words ‘Hello’ and ‘Happy’, and such monitoring of pronunciation may promote the development of artificial intelligence for identification. Figure 4e investigates the real-time response of the pressure sensor during finger pressing and the signal strength of the sensor increases as the pressure increases. In addition, attaching the piezoresistive sensor under the feet can be used to monitor movements with different frequencies such as slow walking, fast walking, and running (Fig. 4f).

Based on the good flexibility, electrical properties and monitoring applications, piezoresistive sensors can also be used to assemble soft electronic skin for recognizing external pressure and shape. As illustrated in Fig. 4g, we demonstrate a prototype of soft electronic skin composed of  $3 \times 5$  array of piezoresistive sensors. The circuit structure of soft electronic skin can be worn conformally on the forearm (Supplementary Fig. 15). Figure 4g shows the performance of the pressure sensing array. As recorded in subfigures (i), (ii) and (iii), three 500 g weights with different

patterns ‘I’, ‘F’, and ‘E’ are placed on the pressure sensor array, all the weights and positions are detected by the pressure array.

#### Monitoring of human motions with the fully paper-based flexible piezoresistive sensor under high-humidity and underwater conditions

In addition to the above-mentioned applications in the ambient condition, the piezoresistive sensor can be applied in a high-humidity environment and even soaked in water. As shown in Fig. 5a, there is no significant influence on sensing functions of the piezoresistive sensor at different humidity of 38–100%. The enlarged data shows the sensing results under the random bending of the wrist in 10 seconds (Fig. 5a right). As shown in the inset, the device works normally and keeps dry at 84% humidity, which is attributed to its good waterproofness and air permeability. Therefore, this fully paper-based sensor can be used in a variety of scenarios, such as in high-humidity weather like rain, snow, fog, or on sweating and wet skin.

The piezoresistive sensor exhibits sensitivity under water because of its hydrophobic surface. When the water drops on the hydrophobic paper and slides, the droplets will not wet the surface, which proves that the sensor made of hydrophobic paper has good waterproof performance. We explored the signal detection abilities of piezoresistive sensor in air and underwater environments. In Fig. 5b, we applied the weight (50 g) to the sensor in air and under water. The sensor can recognize the pressure signal stably, while the signal value would decrease to a certain extent due to the influence of the inherent buoyancy on the weight under water. The pressure responses of the sensor soaked in water for 1 minute (Fig. 5c) and 40 minutes (Fig. 5d) were recorded by repeatedly placing weights (left: 50 g; right: 200 g) on the sensor. After 40 minutes of underwater testing, the pressure response did not change significantly, which proved the good waterproofness and high performance of the packaging layer, indicating that the sensor can respond continuously in the underwater environment. Further, we used piezoresistive sensors for underwater signal monitoring (Fig. 5f). When worn on the wrist, the sensors can be used to record the clenching data (Fig. 5e) and bending data (Fig. 5g) of the hand in the water. When the sensor is worn on the human body for movement monitoring, the body movement will cause obvious water fluctuations, resulting in a certain signal drift, but the amplitude of small signal drift will not affect the monitoring of body movement.

In summary, we constructed a fully paper-based flexible piezoresistive sensor with low cost, simple process, and rapid preparation by stacking the double 'zig-zag' folded paper with dot surfaces and hydrophobic paper with silver paste. The sensing layer is based on graphene/SWNTs composites, which are synthesized by dip coating composite solution on tissue papers, and can be produced on a large scale. The sensing layer is then folded and simply fabricated as a pressure sensor with high sensitivity under the combined reactions of the angle change of 'zig-zag' folded structures, the mutual squeeze between the dots on the surface, and the reduction of the gap among fibers. The piezoresistive sensor shows high sensitivity ( $12.6 \text{ kPa}^{-1}$  and  $4.3 \text{ kPa}^{-1}$  in the wide linear ranges of 0 to 0.6 kPa and 0.6–60.4 kPa), cyclic stability, low working voltage ( $\sim 0.1 \text{ V}$ ), and fast response time (214 ms). Because of fully paper-based materials, the pressure sensor is biodegradable and can be disposed of simply by incineration to prevent the accumulation of electronic waste. Thanks to the air permeability and waterproofness of the encapsulation layer, the pressure sensors can be worn on human skin and monitor human physiological signals, such as the pulse on wrists, the acoustic sound on throat, the finger pressing, the walking signals on feet, and the bending signals on wrist. At the same time, it can also be applied to soft electronic skin to respond to external force and distribution. In addition, due to the hydrophobicity of the piezoresistive sensor, the sensor can be applied in a wet environment or under water, which greatly reduces the influence of environmental humidity on the sensor. It is expected that such fully paper-based piezoresistive sensors with high sensitivity, low working voltage, fast response, hydrophobicity, air permeability, and biodegradability have great potential for low-cost, green, and flexible electronics shortly.

## METHODS

### Materials

Hydrophobic paper: prepared by methyl trichlorosilane (AR,  $\geq 99\%$ , Shanghai Maclin Biochemical Technology Co., Ltd.) and filter paper (200 mm  $\times$  200 mm, Whatman<sup>TM</sup>); Conductive paper: prepared by aqueous composite solutions of single-walled carbon nanotubes and graphene (Suzhou Tanfeng Graphene Technology Co., Ltd.) and a tissue paper with dotted surface

structure (100% native wood pulp, Shandong Heng'an Paper Industry Co., Ltd.); nanocellulose paper: prepared by sodium hydroxide (AR,  $\geq 96\%$ , Nanjing Wanqing Chemical Industry), urea (AC,  $\geq 99\%$ , Tianjin Damao Chemical Reagent Factory), sulfuric acid (AR,  $\geq 98\%$ , Shanghai Titan Technology Co., Ltd.), cotton linters (DP <500, Hubei Jinhanjiang Refined Cotton Co., Ltd.), deionized water (Merck Direct-Q) and absolute ethyl alcohol (AR, Guangdong Guanghua Technology Co., Ltd.); oily adhesive (Guangzhou Sihai adhesive Co., Ltd.); conductive silver paste (65%, Nanjing Xianfeng Nanomaterials Technology Co., Ltd.); parafilm (PM996, PARAFILM).

### Fabrication of hydrophobic paper

A vacuum oven (Shanghai Yiheng Scientific Instrument Co., Ltd.) was preheated to 45 °C, and a petri dish of 1 g methyl trichlorosilane was covered by a filter paper (10 cm  $\times$  10 cm), then placed them in the vacuum oven at 45 °C for 5 minutes. The hydrophobic and air permeable paper can be prepared through evaporating the methyl trichlorosilane on the fibers of filter paper (Fig. 1a, bottom middle).

### Fabrication of conductive paper

A tissue paper with dotted surface structure (12 mm  $\times$  12 mm) was soaked in commercial conductive solution, simultaneously put in ultrasound for 1 minute to make the conductive components more uniform, and then allowed to dry at 120 °C for 10 minutes in an oven to evaporate the aqueous solution. The paper changed color from black to dark grey. In Supplementary Fig. 1a, we controlled the optimal content of conductive components by varying the number of soaking times. We soaked the paper in conductive for 12 times and then tested its sheet resistance, which tended to stabilize after 10 times. Therefore, we chose conductive paper that was soaked for 10 times as the sensing layer of the sensor. Then we folded the tissue paper into a double 'zig-zag' structure as the sensing layer.

### Fabrication of paper-based sensor and pressure sensing array

Two silicon paper masks, made by laser cutting (LIDE laser cutting machine) a 0.2-mm-thick silicon paper film (RUSPEPA nonstick silicone paper), were laminated over the upper and bottom hydrophobic paper, respectively. Then, the silver paste interconnects (1 mm in width and 20  $\mu\text{m}$  in thickness) were screen-printed over the silicon paper mask using a razor blade. Removing the silicon paper mask left solidified silver interconnects' traces on the hydrophobic paper. Two pieces of hydrophobic paper were placed as the packaging layers and the silver paste side was contacted with the conductive paper. The edge of the fabricated piezoresistive sensor was glued by waterproof oily adhesive<sup>74</sup> and formed as hydrophobic-conductive-hydrophobic sandwich layers. The pressure sensing array was fabricated by 3  $\times$  5 piezoresistive sensors and encapsulated by transparent nano-cellulose paper. The preparation process of the transparent nano-cellulose paper refers to the previous work of our group<sup>42,75</sup> (Fig. S2a). Both the piezoresistive sensor and the pressure sensing array were then connected to an external power source and data acquisition system using copper wires.

### Characterization of the paper-based piezoresistive sensor

Pictures of the sensing layer and the final device were obtained using an optical camera. The double 'zig-zag' shape of the folded sensing layer was observed by an optical microscope. The surface structure of the hydrophobic paper and conductive paper was observed by scanning electron microscope (SEM; JSM-7800F, JEOL, Inc.). The resistance on the sensing layer was measured with a four-point probe instrument (ST2253, Suzhou Jingge Electronics Co., Ltd.).

## Monitoring of physical signals at the ambient, high-humidity, and underwater conditions

The resistance data was collected by an electrochemical workstation (Shanghai Chenhua Instrument Co., Ltd.), and the working voltage was set to 0.1 V (Fig. S3). When testing at high humidity and underwater, the external equipment wires were protected with waterproof tape. The external pressure signals were tested by applying a series of metal weights on the top of the sensor. The random touch signals were tested by the fingers touching under different forces. The piezoresistive sensors were also worn on the wrist, throat, back, body joints and sole by band-aid to monitor an adult's pulse, pronunciation, sitting posture, bending response and walking signals, respectively.

## DATA AVAILABILITY

The data that support the findings of this study are available from the corresponding author upon reasonable request.

Received: 22 October 2022; Accepted: 14 February 2023;

Published online: 11 March 2023

## REFERENCES

- Gao, Y. et al. Wearable sensors: Flexible hybrid sensors for health monitoring: Materials and mechanisms to render wearability. *Adv. Mater.* **32**, 2070117 (2020).
- Lim, H.-R. et al. Advanced soft materials, sensor integrations, and applications of wearable flexible hybrid electronics in healthcare, energy, and environment. *Adv. Mater.* **32**, 1901924 (2020).
- Wang, Y. et al. Self-powered wearable pressure sensing system for continuous healthcare monitoring enabled by flexible thin-film thermoelectric generator. *Nano Energy* **73**, 104773 (2020).
- Shi, C. et al. Heterogeneous integration of rigid, soft, and liquid materials for self-healable, recyclable, and reconfigurable wearable electronics. *Sci. Adv.* **6**, eabd0202 (2020).
- Kim, J. et al. Wearable biosensors for healthcare monitoring. *Nat. Biotechnol.* **37**, 389–406 (2019).
- Yokota, T. et al. Recent progress of flexible image sensors for biomedical applications. *Adv. Mater.* **33**, 2004416 (2021).
- Sun, Q. et al. Fully sustainable and high-performance fish gelatin-based triboelectric nanogenerator for wearable movement sensing and human-machine interaction. *Nano Energy* **89**, 106329 (2021).
- Gao, J. et al. Ultra-robust and extensible fibrous mechanical sensors for wearable smart healthcare. *Adv. Mater.* **34**, 2107511 (2022).
- Kim, D.-H. et al. Dissolvable films of silk fibroin for ultrathin conformal bio-integrated electronics. *Nat. Mater.* **9**, 511–517 (2010).
- Shen, Z. et al. Cutaneous ionogel mechanoreceptors for soft machines, physiological sensing, and amputee prostheses. *Adv. Mater.* **33**, 2102069 (2021).
- Lin, S. et al. An ultralight, flexible, and biocompatible all-fiber motion sensor for artificial intelligence wearable electronics. *npj Flex. Electron.* **6**, 27 (2022).
- Kim, D. B. et al. Weave-pattern-dependent fabric piezoelectric pressure sensors based on polyvinylidene fluoride nanofibers electrospun with 50 nozzles. *npj Flex. Electron.* **6**, 69 (2022).
- He, X. et al. Microstructured capacitive sensor with broad detection range and long-term stability for human activity detection. *npj Flex. Electron.* **5**, 17 (2021).
- Zeng, X. et al. Tunable, ultrasensitive, and flexible pressure sensors based on wrinkled microstructures for electronic skins. *ACS Appl. Mater. Interfaces* **11**, 21218–21226 (2019).
- Fang, Y. et al. Deep learning assisted on-mask sensor network for adaptive respiratory monitoring. *Adv. Mater.* **34**, 2200252 (2022).
- Meng, K. et al. Wearable pressure sensors for pulse wave monitoring. *Adv. Mater.* **34**, 2109357 (2022).
- Yi, Z. et al. Piezoelectric dynamics of arterial pulse for wearable continuous blood pressure monitoring. *Adv. Mater.* **34**, 2110291 (2022).
- Lee, S. et al. Nanomesh pressure sensor for monitoring finger manipulation without sensory interference. *Science* **370**, 966–970 (2020).
- Gao, Y. et al. Wearable microfluidic diaphragm pressure sensor for health and tactile touch monitoring. *Adv. Mater.* **29**, 1701985 (2017).
- Boutry, C. M. et al. Biodegradable and flexible arterial-pulse sensor for the wireless monitoring of blood flow. *Nat. Biomed. Eng.* **3**, 47–57 (2019).
- Lee, G.-H. et al. Parallel signal processing of a wireless pressure-sensing platform combined with machine-learning-based cognition, inspired by the human somatosensory system. *Adv. Mater.* **32**, 1906269 (2020).
- Zheng, Q. et al. Graphene-based wearable piezoresistive physical sensors. *Mater. Today* **36**, 158–179 (2020).
- Roh, E. et al. A solution-processable, omnidirectionally stretchable, and high-pressure-sensitive piezoresistive device. *Adv. Mater.* **29**, 1703004 (2017).
- Wang, Z. et al. Highly sensitive integrated flexible tactile sensors with piezoresistive Ge<sub>2</sub>Sb<sub>2</sub>Te<sub>5</sub> thin films. *npj Flex. Electron.* **2**, 17 (2018).
- Park, D. Y. et al. Self-powered real-time arterial pulse monitoring using ultrathin epidermal piezoelectric sensors. *Adv. Mater.* **29**, 1702308 (2017).
- Ouyang, H. et al. A bioresorbable dynamic pressure sensor for cardiovascular postoperative care. *Adv. Mater.* **33**, 2102302 (2021).
- Chen, C. et al. 3D double-faced interlock fabric triboelectric nanogenerator for bio-motion energy harvesting and as self-powered stretching and 3D tactile sensors. *Mater. Today* **32**, 84–93 (2020).
- Wang, C. et al. An ultra-sensitive and wide measuring range pressure sensor with paper-based cnt film/interdigitated structure. *Sci. China Mater.* **63**, 403–412 (2019).
- Su, Z. et al. Designed biomass materials for “green” electronics: A review of materials, fabrications, devices, and perspectives. *Prog. Mater. Sci.* **125**, 100917 (2022).
- Awasthi, A. K. et al. Circular economy and electronic waste. *Nat. Electron.* **2**, 86–89 (2019).
- Xu, Y. et al. Paper-based wearable electronics. *iScience* **24**, 102736 (2021).
- Fan, W. et al. Machine-knitted washable sensor array textile for precise epidermal physiological signal monitoring. *Sci. Adv.* **6**, eaay2840 (2020).
- Lou, M. et al. Hierarchically rough structured and self-powered pressure sensor textile for motion sensing and pulse monitoring. *ACS Appl. Mater. Interfaces* **12**, 1597–1605 (2020).
- Li, S. et al. A skin-like pressure- and vibration-sensitive tactile sensor based on polyacrylamide/silk fibroin elastomer. *Adv. Funct. Mater.* **32**, 2111747 (2022).
- Li, D. et al. Superomniphobic silk fibroin/ag nanowires membrane for flexible and transparent electronic sensor. *ACS Appl. Mater. Interfaces* **12**, 10039–10049 (2020).
- Han, Y. et al. Fish gelatin-based triboelectric nanogenerator for harvesting bio-mechanical energy and self-powered sensing of human physiological signals. *ACS Appl. Mater. Interfaces* **12**, 16442–16450 (2020).
- Zhang, Y. et al. Flexible electronics based on micro/nanostructured paper. *Adv. Mater.* **30**, 1801588 (2018).
- Lin, Y. et al. Recent advancements in functionalized paper-based electronics. *ACS Appl. Mater. Interfaces* **8**, 20501–20515 (2016).
- Xu, Y. et al. Pencil-paper on-skin electronics. *Proc. Natl Acad. Sci. U. S. A.* **117**, 18292–18301 (2020).
- Say, M. G. et al. Spray-coated paper supercapacitors. *npj Flex. Electron.* **4**, 14 (2020).
- Wang, C. et al. Toward scalable fabrication of electrochemical paper sensor without surface functionalization. *npj Flex. Electron.* **6**, 12 (2022).
- Gao, L. et al. All paper-based flexible and wearable piezoresistive pressure sensor. *ACS Appl. Mater. Interfaces* **11**, 25034–25042 (2019).
- Selamneni, V. et al. Large-area, flexible sns/paper-based piezoresistive pressure sensor for artificial electronic skin application. *IEEE Sens. J.* **21**, 5143–5150 (2021).
- Tao, L.-Q. et al. Graphene-paper pressure sensor for detecting human motions. *ACS Nano* **11**, 8790–8795 (2017).
- Liu, X. et al. Paper-based piezoresistive mems sensors. *Lab Chip* **11**, 2189–2196 (2011).
- Sundriyal, P. et al. Inkjet-printed electrodes on a4 paper substrates for low-cost, disposable, and flexible asymmetric supercapacitors. *ACS Appl. Mater. Interfaces* **9**, 38507–38521 (2017).
- Zhan, Z. et al. Paper/carbon nanotube-based wearable pressure sensor for physiological signal acquisition and soft robotic skin. *ACS Appl. Mater. Interfaces* **9**, 37921–37928 (2017).
- Zhang, H. et al. A smart ball sensor fabricated by laser kirigami of graphene for personalized long-term grip strength monitoring. *npj Flex. Electron.* **6**, 28 (2022).
- Chen, S. et al. Flexible and highly sensitive resistive pressure sensor based on carbonized crepe paper with corrugated structure. *ACS Appl. Mater. Interfaces* **10**, 34646–34654 (2018).
- Jo, S. et al. Antibacterial and soluble paper-based skin-attachable human motion sensor using triboelectricity. *ACS Sustain. Chem. Eng.* **8**, 10786–10794 (2020).
- Miyamoto, A. et al. Inflammation-free, gas-permeable, lightweight, stretchable on-skin electronics with nanomeshes. *Nat. Nanotechnol.* **12**, 907–913 (2017).
- Dong, L. et al. Breathable and wearable energy storage based on highly flexible paper electrodes. *Adv. Mater.* **28**, 9313–9319 (2016).
- Yang, W. et al. Air-permeable and washable paper-based triboelectric nanogenerator based on highly flexible and robust paper electrodes. *Adv. Mater. Technol.* **3**, 1800178 (2018).



54. Thiagarajan, K. et al. Flexible, highly sensitive paper-based screen printed mwcnt/pdms composite breath sensor for human respiration monitoring. *IEEE Sens. J.* **21**, 13985–13995 (2021).
55. Liu, H. et al. Paper-based flexible strain and pressure sensor with enhanced mechanical strength and super-hydrophobicity that can work under water. *J. Mater. Chem. C.* **10**, 3908–3918 (2022).
56. Duan, Z. et al. Integrated cross-section interface engineering and surface encapsulating strategy: A high-response, waterproof, and low-cost paper-based bending strain sensor. *J. Mater. Chem. C.* **9**, 14003–14011 (2021).
57. Lee, T. et al. All paper-based, multilayered, inkjet-printed tactile sensor in wide pressure detection range with high sensitivity. *Adv. Mater. Technol.* **7**, 2100428 (2022).
58. Zhu, J. et al. A paper-based self-inductive folding displacement sensor for human respiration and motion signals measurement. *npj Flex. Electron.* **6**, 67 (2022).
59. Liu, L. et al. Bioinspired, superhydrophobic, and paper-based strain sensors for wearable and underwater applications. *ACS Appl. Mater. Interfaces* **13**, 1967–1978 (2021).
60. Yang, T. et al. Paper-based mechanical sensors enabled by folding and stacking. *ACS Appl. Mater. Interfaces* **11**, 26339–26345 (2019).
61. Han, Z. et al. Ultralow-cost, highly sensitive, and flexible pressure sensors based on carbon black and airlaid paper for wearable electronics. *ACS Appl. Mater. Interfaces* **11**, 33370–33379 (2019).
62. Wang, Y. et al. Hierarchically patterned self-powered sensors for multifunctional tactile sensing. *Sci. Adv.* **6**, eabb9083 (2020).
63. Pal, A. et al. Early detection and monitoring of chronic wounds using low-cost, omniphobic paper-based smart bandages. *Biosens. Bioelectron.* **117**, 696–705 (2018).
64. Ouyang, H. et al. Self-powered pulse sensor for antidiastole of cardiovascular disease. *Adv. Mater.* **29**, 1703456 (2017).
65. Jiang, Y. et al. A flexible and ultra-highly sensitive tactile sensor through a parallel circuit by a magnetic aligned conductive composite. *ACS Nano* **16**, 746–754 (2022).
66. Schwartz, G. et al. Flexible polymer transistors with high-pressure sensitivity for application in electronic skin and health monitoring. *Nat. Commun.* **4**, 1859 (2013).
67. Luo, C. et al. A new approach for ultrahigh-performance piezoresistive sensor based on wrinkled ppy film with electrospun PVA nanowires as spacer. *Nano Energy* **41**, 527–534 (2017).
68. Hsu, P.-C. et al. Assessment of subtle changes in diabetes-associated arteriosclerosis using photoplethysmographic pulse wave from index finger. *J. Med. Syst.* **42**, 43 (2018).
69. Argyropoulou, O. D. et al. Accelerated atheromatosis and arteriosclerosis in primary systemic vasculitides: Current evidence and future perspectives. *Curr. Opin. Rheumatol.* **30**, 36–43 (2018).
70. Oliver, M. F. et al. Management of acute myocardial infarction. *Lancet* **383**, 409–410 (2014).
71. Houston, M. The role of noninvasive cardiovascular testing, applied clinical nutrition and nutritional supplements in the prevention and treatment of coronary heart disease. *Ther. Adv. Cardiovasc. Dis.* **12**, 85–108 (2018).
72. Jin, K. et al. Telehealth interventions for the secondary prevention of coronary heart disease: A systematic review and meta-analysis. *Eur. J. Cardiovasc. Nurs.* **18**, 260–271 (2019).
73. Ezzati, M. et al. Contributions of risk factors and medical care to cardiovascular mortality trends. *Nat. Rev. Cardiol.* **12**, 508–530 (2015).
74. Liu, S. et al. Rollerball-pen-drawing technology for extremely foldable paper-based electronics. *Adv. Electron. Mater.* **3**, 1700098 (2017).
75. Gao, L. et al. Flexible, transparent nanocellulose paper-based perovskite solar cells. *npj Flex. Electron.* **3**, 4 (2019).

## ACKNOWLEDGEMENTS

This work was financially supported by the Joint Research Funds of Department of Science & Technology of Shaanxi Province and Northwestern Polytechnical University (No. 2020GXHLH-Z-021), and Fundamental Research Funds for the Central Universities.

## AUTHOR CONTRIBUTIONS

All authors contributed to the preparation of this manuscript. Y.W.W. and H.D.Y. conceived the original idea and designed the research. C.Q.S., H.D.Y., and W.H. supervised the overall project. X.W.S. and Y.W.W. conducted the experiments and drew the figures. Y.W.W., X.W.S., L.X.H., J.C.Z., and Z.Q.Y. performed device and material characterization.

## COMPETING INTERESTS

The authors declare no competing interests.

## ADDITIONAL INFORMATION

**Supplementary information** The online version contains supplementary material available at <https://doi.org/10.1038/s41528-023-00244-5>.

**Correspondence** and requests for materials should be addressed to Chuanqian Shi, Hai-Dong Yu or Wei Huang.

**Reprints and permission information** is available at <http://www.nature.com/reprints>

**Publisher's note** Springer Nature remains neutral with regard to jurisdictional claims in published maps and institutional affiliations.



**Open Access** This article is licensed under a Creative Commons Attribution 4.0 International License, which permits use, sharing, adaptation, distribution and reproduction in any medium or format, as long as you give appropriate credit to the original author(s) and the source, provide a link to the Creative Commons license, and indicate if changes were made. The images or other third party material in this article are included in the article's Creative Commons license, unless indicated otherwise in a credit line to the material. If material is not included in the article's Creative Commons license and your intended use is not permitted by statutory regulation or exceeds the permitted use, you will need to obtain permission directly from the copyright holder. To view a copy of this license, visit <http://creativecommons.org/licenses/by/4.0/>.

© The Author(s) 2023